Seismic Performance of Cold-Formed Steel Framed Shear Walls using In-Frame Corrugated Steel Sheathing

Zhang W.[1], Lan X.[2], Mahdavian M.[3], Yu C.[4]

Abstract

To meet the increasing demand for high strength and non-combustible shear wall systems in mid-rise cold-formed steel (CFS) constructions, an innovative CFS shear wall system with in-frame corrugated steel sheathing is invented and investigated in this paper experimentally and numerically. Bearing wall and shear wall specimens with in-frame corrugated steel sheathing are tested under combined lateral and gravity loading. The results show that the shear strength of the innovative shear wall is higher than currently code certified shear walls in AISI S400 so that it could be employed for mid-rise buildings in areas that are prone to high seismic, and wind loads more efficiently. It is also found that the shear strength of bearing walls is approximately one-third of the shear strength of shear walls, which proves that bearing walls also provide significant shear resistance in a structure. To evaluate and quantify the seismic performance factors of this new lateral force-resisting system, nonlinear static and dynamic analyses are performed on 6 building archetypes by using OpenSees software according to the methodology recommended by FEMA P695. The seismic performance evaluation results verified that the existing seismic performance factors used for light-framed shear wall systems with flat steel sheets can also be used for the innovative cold-formed steel shear wall system.

1. Introduction

Mid-rise cold-formed steel (CFS) framed structures are one of the economic solutions for the increasing housing demand, especially in highly populated areas. Due to the non-combustibility material requirement by the International Building Code (IBC 2015) for Types I and II constructions, shear walls with flat steel sheets and cross bracing shear walls are the only available options for mid-rise buildings. However, the low strength of the shear wall with flat steel sheets significantly obstructs the application of cold-formed steel in mid-rise buildings, particularly in areas subjected to high seismic and/or strong wind hazards. Whereas the cross-bracing shear wall has a relatively lower response modification factor of 4.0. Non-combustible CFS shear walls with high structural performance are in great need in the mid-rise construction field.

---

[1] Associate Professor, Beijing University of Technology, <zhangwy@bjut.edu.cn>
[2] Graduate Research Assistant, University of North Texas, <xing.lan1992@gmail.com >
[3] Engineer, ASC Steel Deck, <mahsa.mahdavian@ascsteeldeck.com>
[4] Professor, University of North Texas, <cheng.yu@unt.edu>

Replacing flat sheet panels with corrugated steel sheets is a solution to improve shear walls' strength. Shear walls with corrugated steel sheets have been a subject of interest for multiple researchers in recent years. These researchers have investigated a wide range of parameters and their effects on the lateral performance of the shear walls such as: sheathing and framing thickness (Stojadinovic and Tipping 2007, Yu et al. 2009), fastener size and spacing (Stojadinovic and Tipping 2007), wall aspect ratio (Mahdavian 2016), opening patterns on corrugated steel sheathing (Yu 2013, Yu et al., 2016, Mahdavian 2016), gravity loads (Mahdavian 2016, Zhang et al., 2017a), etc. All the experimental results indicated that shear walls with corrugated steel sheets have the characteristics of high strength and stiffness. The shear walls investigated by the prementioned researchers has the corrugated steel sheathing attached to the surface of the framing members (referred as sheet-out shear walls, shown in Figure 1a) causing unequal wall thickness with adjacent walls, which would cause difficulty creating a smooth surface for wall finishes. Therefore, Zhang et al. (2021) proposed a new shear wall system with the corrugated steel sheathing placed inside the framing members, referred as in-frame/sheet-in shear walls. A total of three shear wall configurations were investigated and it was concluded that sheet-in shear wall with a low-profile single vertical track placed at wall center (as shown in Figure 1b) demonstrated high shear strength and good ductility.
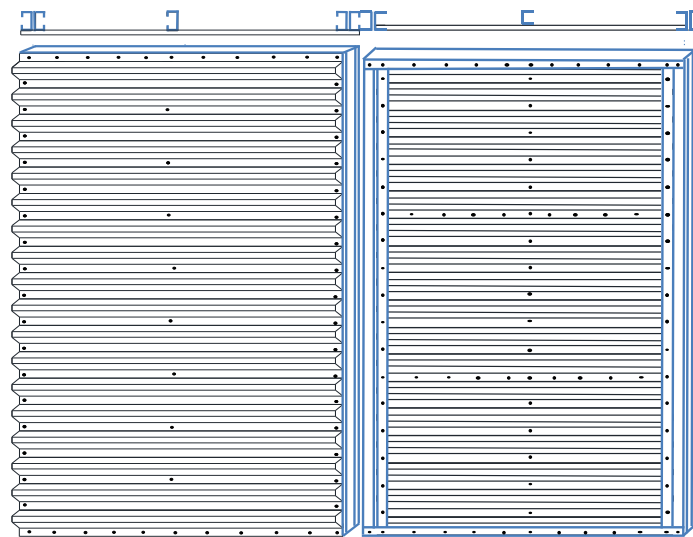
Figure 1: Schematic drawing of (a) sheet-out shear walls; (b) in-frame shear walls

This paper is continuing research after Zhang et al. (2021) research and intends to provides a practical design method of this innovative shear wall system. The research started with testing of both shear wall and bearing wall specimens under combined lateral and gravity loading. Subsequently, seismic performance evaluations are performed on office and hotel building archetypes with the innovative in-frame shear wall systems following FEMA P695 (2009) methodology. Details of the experiments and finite element analysis results are reported.

2. Test Program

2.1 Test Setup
All tests were conducted on a 4.88 m by 3.66 m (16 ft. by 12 ft.) high-self-equilibrating steel testing frame. The testing frame was equipped with an MTS 156 kN (35 kip) hydraulic actuator with a 254 mm (10 in.) stroke. The lateral force was applied to the top of the wall by a hydraulic actuator

through a 'T' shaped steel beam. A 133 kN (30 kip) universal compression/tension load cell was used to measure the applied forces. For shear wall specimens, two Simpson Strong-Tie S/HD15S hold-downs were used at each end of the wall. The hold down bolts used two F3125 Grade A490 (2019) bolt with 19.1mm (3/4 in.) diameter. Two additional F3125 Grade A325 (2019) shear bolts with 15.9mm (5/8 in.) diameter were used to anchor the bottom track to the base beam. No hold down was installed for bearing wall specimens, and four shear bolts were used to anchor the bearing wall specimens to the base beam. One out of five position transducers were used to measure the horizontal displacement at the top of the shear wall, and the other four were used to measure the vertical and horizontal displacements at the bottom of the two boundary frame members. In all tests, a constant 24 kN (5,384 lbs) gravity load was applied to the top of the wall by two weight boxes, one on each side of the wall. Contact between weight boxes and wall specimens was eliminated by a supporting frame. Details of the test setup and arrangement of the position transducers are shown in Figure 2.

2.2 Test Method
Both monotonic and cyclic tests were conducted. The procedure of the monotonic tests is by ASTM E564 "Standard Practice for Static Load Test for Shear Resistance of Framed Walls for Buildings" (2012). The displacement was applied to the top of the wall at a uniform rate of 0.19 mm/s (0.0075 in./s). The cyclic tests adopted the CUREE protocol with 0.2 Hz (5 seconds) loading frequency, which is by Method C in ASTM E2126 "Standard Test Methods for Cyclic (Reversed) Load Test for Shear Resistance of Vertical Elements of the Lateral Force Resisting Systems for Buildings" (2006). To determine the post-peak behavior of the walls, three additional cycles were added to the standard test method.

2.3 Test Specimens
The in-frame corrugated steel sheathing configuration used two track members as the chord studs at each end of the wall specimens, as they allow the installation of corrugated steel sheets within the wall frame. A slightly wider track member was used at the top and bottom of the wall. Two types of walls were investigated in this research: the shear wall and the bearing wall. The sheathings used three individual Verco Decking SV36 sheets with 0.69 mm (27 mils) thickness placed on one side. The cross-section of the corrugated steel sheet is shown in Figure 3. The details of the wall specimens are summarized in Table 1 and Figure 4.
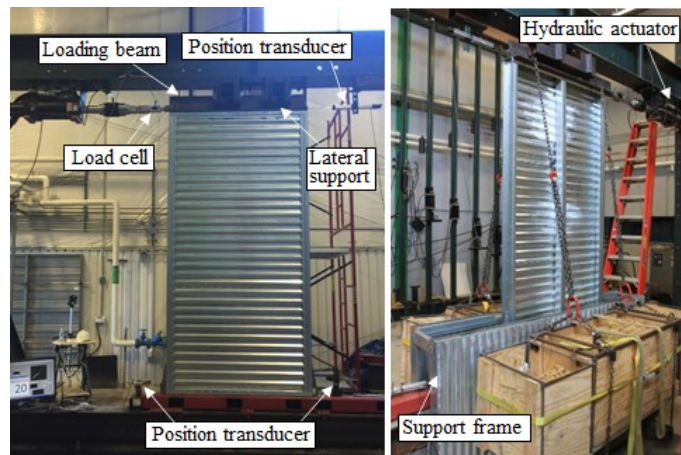
Figure 2: Test Setup: (a) Test specimen without gravity load (b) Test specimen with gravity load

3

Table 1: Test Matrix

Test Label	Wall Type	End Studs	Interior Stud	Horizontal Track	Test protocol (M/C)	Hold-down
BW-M-T1	Bearing wall	350T125-68	300T200-68	362T150-68	M	N
BW-C-T1	Bearing wall	350T125-68	300T200-68	362T150-68	C	N
BW-C-T2	Bearing wall	350T125-68	300T200-68	362T150-68	C	N
SW-M-T1	Shear wall	(2)350T125-68	300T200-68	362T150-68	M	Y
SW-C-T1	Shear wall	(2)350T125-68	300T200-68	362T150-68	C	Y
SW-C-T2	Shear wall	(2)350T125-68	300T200-68	362T150-68	C	Y

Note: M - Monotonic loading, C - Cyclic loading.
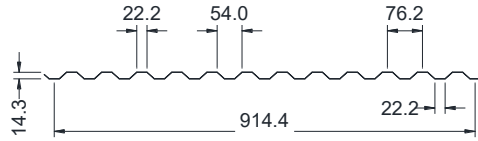
Figure 3: Verco Decking SV36 Sheathing Profile (unit: mm)
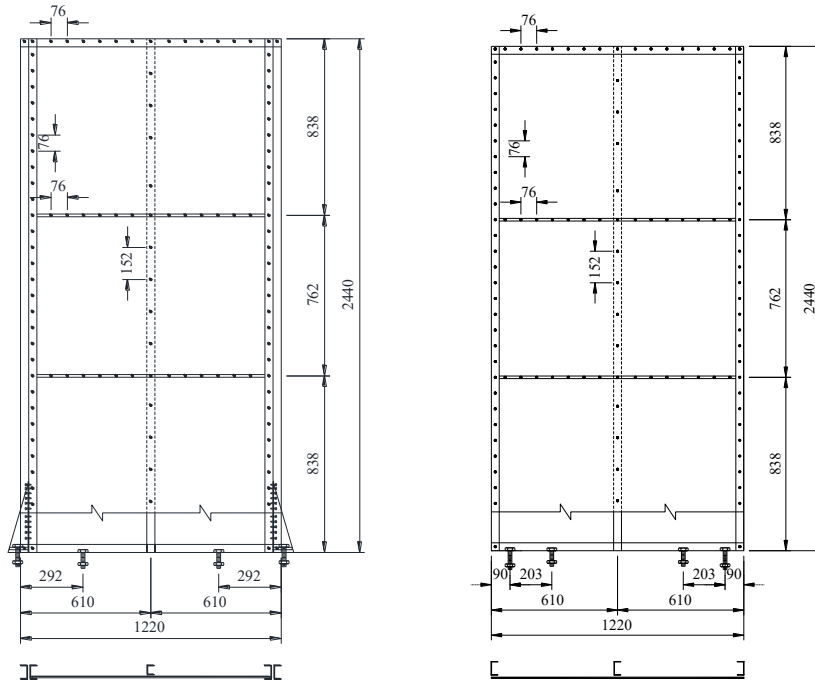
Figure 4: Schematic Drawings of (a) Shear Walls; (b) Bearing Walls (unit: mm)

2.4 Material Properties

Coupon tests were conducted according to the ASTM A370 "Standard Test Methods and Definitions for Mechanical Testing of Steel Products" (2006) to obtain the actual properties of all test materials. The coating of the steel samples was removed before coupon tests. A total of three coupon tests were performed for each type of member, and the average results are provided in Table 2.

Table 2: Material Properties of Wall Components

Member	Uncoated Thickness (mm)	Yield Stress Fy (MPa)	Tensile Strength Fu (MPa)	Fy/Fu	Elongation for 50 mm (2 in.) Gage Length (%)
362T150-68	1.831	366.5	483.1	1.32	20.1
350T125-68	1.806	396.4	513.1	1.29	26.1
300T200-68	1.803	379.2	490.0	1.29	29.8
0.69mm Verco Decking SV36	0.729	593.6	620.0	1.04	6.2

3. Test Results and Discussions

3.1 Bearing Wall

For the test of bearing wall under monotonic loading, it was observed that the vertical chord tracks and the bottom horizontal track on the tension side were lifted as soon as the loading started. The bottom of the vertical chord track buckled and the wall reached its peak load as the displacement increased to 2.7% drift (65 mm, 2.6 in.). Buckling on the bottom horizontal track was also noticed. The buckling of the vertical chord track and bottom horizontal track aggravated as the loading continued. No obvious sheathing deformation or screw failure observed after the loading was terminated. The maximum applied lateral displacement was set to 7.5% story drift i.e., was 182.9 mm (7.2 in.). The bearing wall specimen was able to carry the gravity load without collapse during the entire loading process. The failures of the bearing wall specimen under monotonic loading are shown in Figure 5(a).

For bearing wall specimens under cyclic loading, significant vertical displacement of the chord track was observed at the bottom of the frame since no hold down was installed. The vertical chord tracks buckled at the bottom end at the peak cycle. The main failure mode was the local crushing of vertical chord tracks accompanied by local buckling of the horizontal bottom track. Unlike bearing walls in the monotonic test, screws pull-out was observed at the vertical chord track to horizontal track connection. Maximum drift in the cyclic test reached 4.79% and it was concluded that bearing walls were able to carry gravity load without collapse during the test. The failures of the bearing wall specimen in the cyclic test are shown in Figure 5(b)-(c).

(a) Deformations after the loading process

(b)Local crushing of vertical chord tack and horizontal track buckling; (c) Screw pull-out
Figure 5: Failures of Bearing Wall

3.2 Shearing Wall

For the shear wall test under monotonic loading, no significant vertical displacement was detected due to the anchorage of hold-downs. The main failure mode was local buckling in the vertical chord tracks at the compression side right above the hold-down area. Local damage to the intermediate interior vertical track was also observed as the displacement increased and a tension field gradually developed along the diagonal direction of the sheathing. The loading was terminated at 7.5% drift and the shear walls were capable of carrying the gravity load without collapse during the entire loading process. Screw pull-out failures on the bottom corrugated steel sheathing were noticed after the wall was unloaded. The failures of the shear wall specimen in the monotonic test are shown in Figure 6(a)-(b).

The behavior of shear wall specimens in the cyclic tests was almost the same as that observed in the monotonic test. The two vertical chord tracks buckled right above the hold-down at the 35th and the 38th cycles (2.9% and 3.3% drift), respectively. As the loading continued, the deformation on the sheathings developed gradually, and screw connection failure occurred on the bottom sheathing, either by screw shear or screw pull-out failure. Buckling of the interior vertical track was also observed. The failures of the shear wall specimen under cyclic loading are shown in Figure 6(c)-(d).

(a) Vertical chord tracks buckling   (c) Sheathing deformation (monotonic)

| (b) Screw pull-out | (d) Sheathing deformation(cyclic) |

Figure 6: Failures of the Shear Wall

3.3 Test Data Results and Discussions

Typical test curves under monotonic and cyclic loading are shown in Figure 7. As can be seen, for bearing wall specimens, the load-displacement curve under monotonic loading almost coincides with the test curve under cyclic loading in the first quadrant. The loading method seemed have no impact on the shear capacity of the bearing wall specimens. As for shear wall specimens, the load-displacement curve under monotonic loading was a bit lower than the test curve under cyclic loading in the first quadrant, and the peak displacement was brought forward. The load-displacement curves of all wall specimens were almost linear at the beginning of the loading, and entered in to the non-linear stage at about 40-50% of the peak load. The shear capacities of the wall specimens dropped significantly after the peak load, indicating ultimate failure of the wall specimens.

The data results of each specimen are provided in Table 3. According to Table 3, the shear capacity and the initial stiffness of bearing wall specimens were 36% and 42% on average of that of the shear wall specimens, respectively. Considering the number of bearing walls in CFS framed buildings, their contributions to the lateral force-resisting can be significant. Therefore, including of bearing walls is highly necessary for the simulation of the building systems.
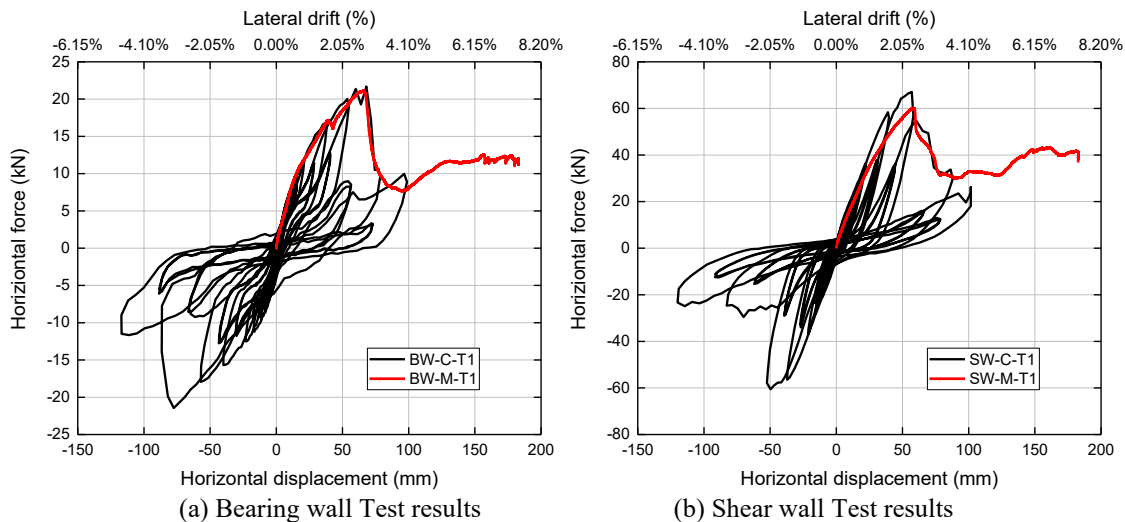
| (a) Bearing wall Test results | (b) Shear wall Test results |

Figure 7: Test Curves

Table 3: Results of Each Wall Specimen

Test label	P_{max} (kN)	Δ_{max} (mm)	F_{nom} (kN/m)	K (kN/m)	P_y (kN)	Δ_y (mm)	P_u (kN)	Δ_u (mm)	Ductility Factor
BW-M-T1	21.1	65.6	16.9	687	17.3	25.2	16.9	69.6	2.760
BW-C-T1	24.6	76.7	17.4	519	19.9	38.1	19.7	86.6	2.295
BW-C-T2	21.6	72.7	16.0	810	17.6	22.3	17.3	86.5	4.075
SW-M-T1	60.2	58.4	49.3	1488	51.7	34.8	48.1	62.8	1.808
SW-C-T1	61.6	53.8	50.5	1535	55.3	36.2	49.3	66.8	1.843
SW-C-T2	63.8	53.4	52.3	1830	56.6	31.0	51.0	59.7	1.928

Table 4: Shear strength comparisons (kN/m)

Sheathing materials	12 mm 4-ply Structural 1 plywood	11 mm OSB	In-frame corrugated sheet
Shear strength	41.1	31.6	50.7

Nominal shear strength results from the conducted tests are compared with code certified wood-based panel shear walls in AISI S400(2015), as shown in Table 4. As we can see, the shear strength of a shear wall with 0.69 mm in-frame corrugated steel sheathing is 64% and 25% greater than that of the plywood and OSB sheathed shear walls, respectively. Therefore, the shear wall with in-frame corrugated steel sheathing is an efficiently lateral force resisting system and could be employed for mid-rise CFS buildings.

4. Finite Element Modeling

4.1 Building Archetypes
This study adopted the office and hotel archetype models in Zhang et al. (2017 b) for seismic performance analysis. The key archetype design parameters are summarized in Table 5. The following assumptions were used in the archetype design:

(1) Building occupancy: The hotel building archetype has a plan dimension of 20.30 m × 15.19 m (66.6 ft. × 49.8 ft.). The shear walls were placed on the exterior of the building. The bearing walls are designed in the interior of the building. Figure 8 illustrates the plan layouts of these two building archetypes.
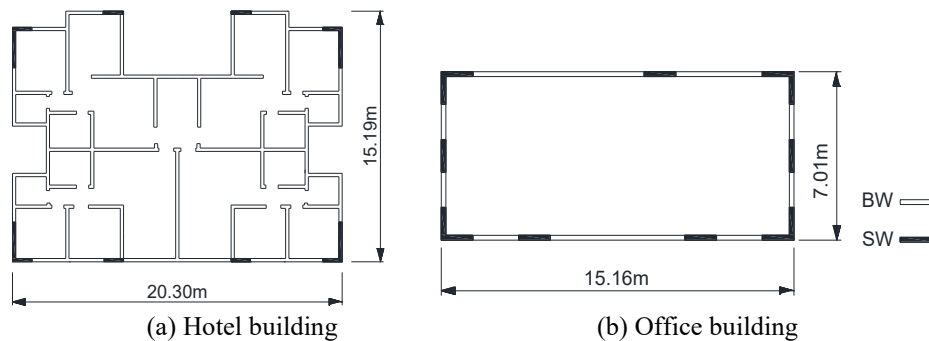
(a) Hotel building   (b) Office building
Figure 8: Building Archetype Plan Layouts

(2) Number of stories: Building stories vary from 2-story to 5-story. Per Table 504.4 in IBC (2015), light-framed buildings constructed with noncombustible material can increase the building height from 3 stories to 5 stories. As a result, 5-story is considered as the maximum story for both building archetypes.

(3) Seismic design category (SDC): The archetypes are assumed to be designed in SDC D per ASCE 7(2016). The Maximum Considered Earthquake (MCE) spectral response acceleration parameter for short-period S_{ms}=1.5g is used for the hotel structure and S_{ms}=1.39g for the office structure.

(4) Design Criteria: Load Resistance Factor Design (LRFD) was applied in the design of the lateral force-resisting system. The seismic force modification factors were based on the light-frame steel shear resistance systems with flat steel sheathing (ASCE7 2016), i.e., R = 6.5, Ω = 3.0, and C_d=6.5. These factors were initially assumed in the building archetype design and were subject to be evaluated in this study.

Table 5: Two Groups of Building Archetypes

Group	Arch. ID	No. of Stories	Key Archetype Design Parameters				
			Occupancy	Shear Wall Aspect Ratio	S_{MT}[1] (g)	T[2](s)	V/W[3](g)
Group 1	1	2	Hotel	2.46	1.5	0.262	0.154
	2	4	Hotel	2.46	1.5	0.44	0.154
	3	5	Hotel	2.46	1.5	0.52	0.154
Group 2	4	2	Office	2.57	1.39	0.245	0.143
	5	3	Office	2.57	1.39	0.332	0.143
	6	5	Office	2.57	1.39	0.486	0.143

Notes: 1. S_{MT} - Maximum considered earthquake spectral acceleration.
2. T - Fundamental period calculated according to Section 5.2.5 in FEMA P695(2016).
3. V/W = C_s = The seismic response coefficient.

4.2 Design of Shear Walls
Earthquake loads were calculated according to ASCE 7, and the vertical distribution of seismic forces and the number of shear walls were determined afterward. The nominal shear wall strength was based on the test results reported in this research. It should be noted that the width of the shear wall used in the building archetype was 1.07 m (3.5 ft.) wide, the nominal strength shall be multiplied by (2w/h).   In addition, a resistance factor of ϕ = 0.6 was considered according to the provisions in AISI S400 (2015).

4.2 Modeling of Shear Walls and Bearing Walls
The shear walls were simulated in OpenSees (2021) as two diagonal truss elements and elastic beam-column elements. To achieve the pinching effect of the wall specimens, Pinching4 uniaxial hysteretic material was used for the diagonal truss elements. The complete set of Pinching4 parameters can be found in Table 6. The definition of the parameters can be found in the OpenSees Command Manual. To obtain the backbone curve of Pinching4 material, the relationship between the load and displacement in the horizontal direction was first converted to the stress and strain in the truss elements. The bearing walls were modeled following the same technique as the shear wall models. The complete set of Pinching4 parameters for bearing walls can be found in Table 7.

Figure 9 shows the comparison between the shear wall simulation and the shear wall test results. Only the last 15 cycles of the 43 test cycles are plotted in Figure 9, because they are the most important cycles as the force and displacement of previous cycles are not significant. It can be seen that the simulation results and test results are in good agreement. Also, the OpenSees model can simulate the post-peak behaviors of the wall specimens.

Table 1: Pinching4 material parameters used for shear wall

D1	D2	D3	D4	F1	F2	F3	F4
0.35	0.74	1.0	1.75	0.52	0.89	1.0	0.66
gK1	gK2	gK3	gK4	gKlim	gD1,2	gD3,4	gDlim
-1.0	-0.20	0.20	0.20	0.90	0.40	2.0	0.50
gF1,2	gF3,4	gFlim	rForce	uForce	rDisp		
0.0	0.0	0.0	0.1	-0.1	0.1		

Table 2: Pinching4 material parameters used for bearing wall

D1	D2	D3	D4	F1	F2	F3	F4
0.34	0.86	1.0	1.62	0.65	0.94	1.0	0.72
gK1	gK2	gK3	gK4	gKlim	gD1,2	gD3,4	gDlim
-1.0	-0.20	0.20	0.20	0.90	0.40	2.0	0.50
gF1,2	gF3,4	gFlim	rForce	uForce	rDisp		
0.0	0.0	0.0	0.15	-0.2	0.1		
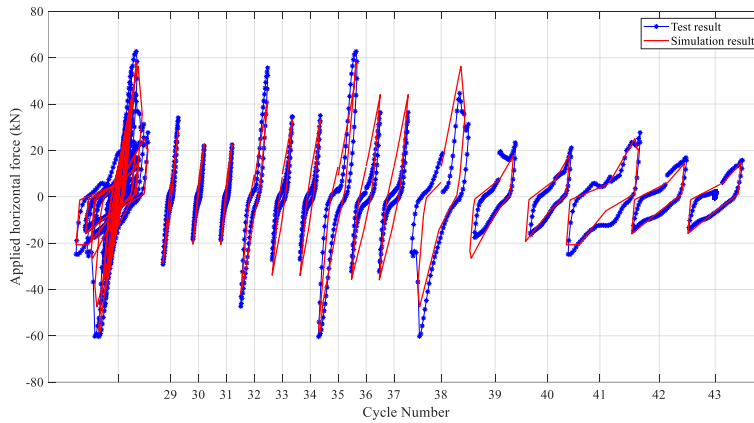
Figure 9 Comparison between Shear Wall Simulation Results and Test Results

4.3 Modeling of Diaphragm, Seismic Mass and Gravity Load

Per the modeling recommendations in Leng (2015) and Zhang et al. (2017 b), this study modeled the floor and roof diaphragms as the rigid. Total seismic mass was referred as the effective seismic mass calculated in the Design Narrative. For the hotel building, the seismic mass was calculated based on ASCE 7 (2016).

4.4 Nonlinear tact (Pushover) Analysis

The applied lateral force at each story level was in proportion to the fundamental mode shape of the index archetype model. The overstrength factor for a given index archetype model is defined as $\Omega_0 = V_{max}/V_{design}$, where V_{max} is the maximum base shear in actual behavior and V_{design} is base shear at design level. The displacement ductility factor is defined as $\mu_T = \delta_u/\delta_{y.eff}$, where displacement, δ_u, is taken as the roof displacement at the point of 20% strength loss (0.8 V_{max}), and the effective yield roof drift displacement $\delta_{y.eff}$ is per Equation 6-7 of FEMA-P695 (2009). Typical pushover curves of the 2-story office building in both directions are shown in Figure 10. The detailed pushover results are summarized in Table 8 and Table 9.

(a) Long Direction   (b) Short Direction
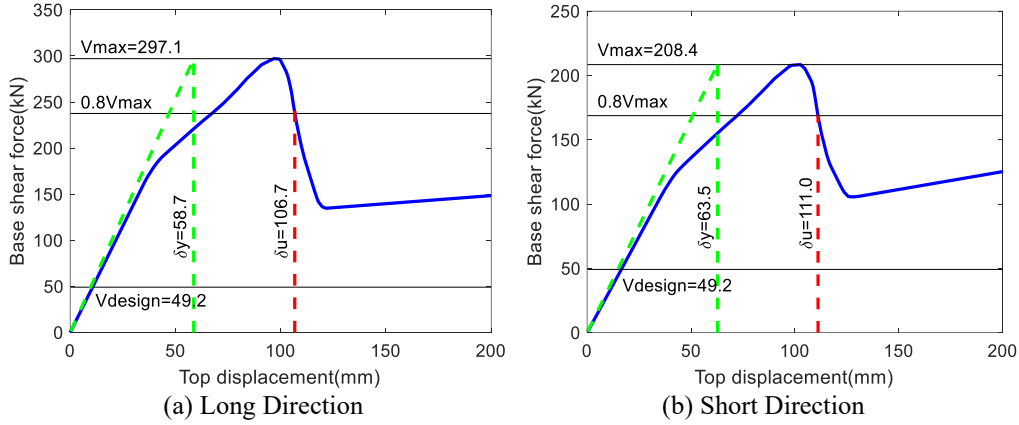
Figure 10: Pushover Curve of the 2-story Office Building

Table 8: Pushover results (long direction)

Occupancy	Height	T (s)	$T1$ (s)	$\delta_u(mm)$	$\delta_{y.eff}$ (mm)	V_{max} (kN)	V_{design} (kN)	μ_T	Ω
Office building	2-story	0.244	0.470	107	59	297	49	1.82	6.04
	3-story	0.332	0.650	151	83	321	78	1.83	4.10
	5-story	0.486	1.117	420	167	361	136	2.52	2.67
Hotel building	2-story	0.262	0.656	116	64	376	78	1.80	4.80
	4-story	0.44	1.131	167	161	608	246	1.04	2.47
	5-story	0.52	1.336	607	202	638	288	3.00	2.22

Table 9: Pushover results (short direction)

Occupancy	Height	T (s)	$T1$ (s)	$\delta_u(mm)$	$\delta_{y.eff}$ (mm)	V_{max} (kN)	V_{design} (kN)	μ_T	Ω
Office building	2-story	0.244	0.580	63	64	49	8	4.24	2.47
	3-story	0.332	0.794	156	97	252	78	1.62	3.22
	5-story	0.486	1.420	466	213	285	136	2.19	2.10
Hotel building	2-story	0.262	0.611	116	64	429	78	1.82	5.48
	4-story	0.44	0.981	133	122	615	246	1.09	2.50
	5-story	0.52	1.072	280	153	751	288	1.83	2.61

4.5 Incremental Dynamic Analysis

In this research, building archetypes were subject to a suite of far-field ground motion records, as suggested by FEMA P695(2009) for collapse evaluation of index archetypes designed for Seismic Design Category B, C, or D. Twenty-two Far-Field records were selected from the Pacific Earthquake Engineering Research Center (PEER) database.

Collapse margin ratio is the primary parameter used to evaluate the collapse safety of the building design. The monotonic test results showed that the sheet-in shear wall could reach 7.5% drift without collapse. As discussed earlier, this study chose 7% as the drift limit for the innovative sheet-in shear wall system in IDA analysis.

The IDA results are plotted by the spectral intensity of the ground motion versus the maximum story drift ratio recorded in the IDA analysis. Figure 11(a) shows the IDA analysis results of the 2-story office building in the long direction. Another expression of the IDA result is the fragility curve. Figure 11(b) shows fragility curve of the 2-story office building in the long direction.
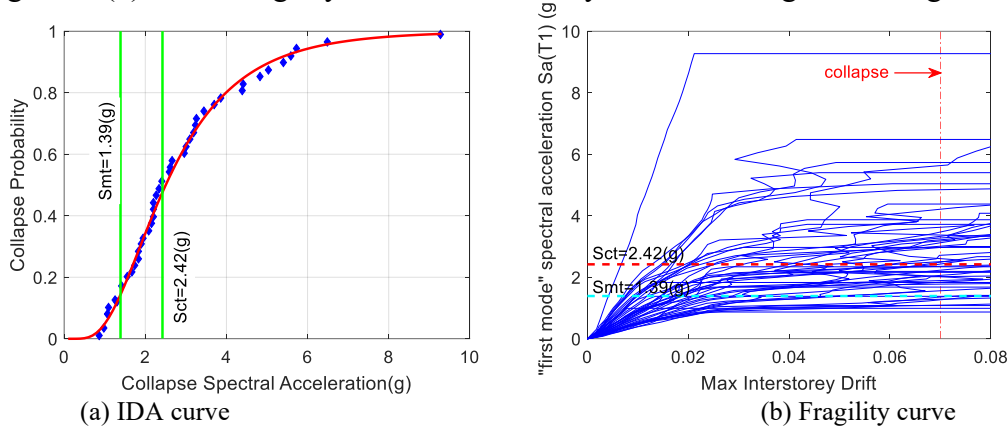
(a) IDA curve   (b) Fragility curve
Figure 11: IDA Results of the 2-Story Office Building in the Long Direction

5. Seismic Performance Evaluation

This section discusses the process of evaluating the seismic performance of this newly proposed sheet-in shear wall seismic-force-resisting system, assessing the acceptable trial value of the response modification coefficient, R, determining appropriate values of the system overstrength factor, Ω_0, and the deflection amplification factor, C_d. The results of the performance evaluation for the office and hotel performance groups are summarized in Table 10.

Table 10: Performance Evaluation Results of the Two Groups of Building Archetypes (Good Uncertainty)

		Ω_0	μ_T	S_{CT}	S_{MT}	CMR	SSF	ACMR	β_{TOT}	Accept ACMR (20%)	Accept ACMR (10%)
Office building	2-story-long	6.04	1.82	2.42	1.39	1.741	1.119	1.948	0.447	1.458	1.775
	2-story-short	4.24	1.77	2.42	1.39	1.741	1.116	1.943	0.444	1.441	1.742
	3-story-long	4.1	1.83	2.83	1.39	2.036	1.12	2.279	0.448	1.458	1.775
	3-story-short	3.22	1.62	2.53	1.39	1.82	1.107	2.015	0.434	1.441	1.742
	5-story-long	2.67	2.52	2.53	1.39	1.82	1.156	2.104	0.494	1.513	1.886
	5-story-short	2.1	2.19	2.31	1.39	1.662	1.141	1.896	0.471	1.485	1.83
Mean of Office Performance Group		3.73	1.96	2.51	1.39	1.803	1.127	2.031	0.456	1.466	1.792
Hotel building	2-story-long	4.8	1.8	2.46	1.5	1.64	1.118	1.834	0.445	1.454	1.768
	2-story-short	5.48	1.82	2.42	1.5	1.613	1.119	1.805	0.447	1.456	1.773
	4-story-long	2.47	1.04	2.35	1.5	1.567	1.02	1.598	0.402	1.402	1.674
	4-story-short	2.5	1.09	2.35	1.5	1.567	1.045	1.637	0.405	1.406	1.68
	5-story-long	2.22	3	2.71	1.5	1.807	1.184	2.139	0.529	1.565	1.97
	5-story-short	2.61	1.83	2.63	1.5	1.753	1.13	1.981	0.447	1.456	1.773
Mean of Hotel Performance Group		3.35	1.76	2.49	1.5	1.658	1.103	1.832	0.446	1.457	1.773

According to the test results by Shafer (2016) the measured damping of the CFS framed building using wood sheathed shear walls varied from 4% to 9%. The authors adopted 5% inherent damping in this research, which was believed to be appropriate. As a result, the damping coefficient, B_I,

equals to 1.0, which makes C_d equal to R. The average value of adjusted collapse margin ratio (ACMR) for each performance group exceeded the corresponding $ACMR_{10\%}$ value. This proved that the trial value of the response modification coefficient, R, 6.5, is acceptable. This study proposed the use of 3.0 for overstrength factor as the average value of each performance group. Lastly, the deflection amplification factor, C_d, was equal to R due to the value of B_I equals to 1.0.

6. Conclusions
In this study, it was the first time to test the sheet-in shear walls under combined lateral and gravity loads. The monotonic and cyclic test results showed local buckling of the chord framing members above the hold-downs. The test results also showed that the strength of the sheet-in bearing wall was approximately one third of the strength of the sheet-in shear wall. If a structure has large number of bearing walls, their contribution to the lateral force resisting system may be utilized. In the monotonic tests, it was observed that both sheet-in bearing wall and shear wall were able to carry gravity load without collapse at the maximum drift of 7.5% so that 7% drift was conservatively set as the collapse drift limit for the innovative sheet-in shear wall in the numerical model.

The seismic performance evaluation was performed on two groups of building archetypes by following the methodology in FEMA P695. Nonlinear static and dynamic analysis were performed in both horizontal directions of each building archetype. The results of the performance evaluation verified the seismic performance factors (R=C_d=6.5 and Ω=3.0) were appropriate for the sheet-in shear wall system based on good uncertainty ratings. It shall be noted that implementation of the methodology in FEMA P695 involves uncertainty, judgment and other variations.

References
AISI S400 (2015). "North American Standard for Seismic Design of Cold-Formed Steel Structural Systems." Washington, D.C.: American Iron and Steel Institute.

ASCE 7 (2016). "Minimum design loads for buildings and other structures." Edition. Reston,VA: American Society of Civil Engineers.

ASTM A325 (2007). "A325-07 Standard Specification for Structural Bolts, Steel, Heat Treated, 120/105 ksi Minimum Tensile Strength." West Conshohocken, PA.: American Society for Testing and Materials.

ASTM A370 (2006). "A370-06 Standard Test Methods and Definitions for Mechanical Testing of Steel Products." West Conshohocken, PA.: American Society for Testing and Materials.

ASTM A490 (2008). "A490-08 Standard Specification for Structural Bolts, Steel, Heat Treated,150 ksi Minimum Tensile Strength." West Conshohocken, PA: American Society for Testing and Materials.

ASTM E2126 (2019). "Standard Test Methods for Cyclic (Reversed) Load Test for Shear Resistance of Vertical Elements of the Lateral Force Resisting Systems for Buildings." West Conshohocken, PA. American Society for Testing and Materials,

ASTM E564 (2012). "Standard Practice for Static Load Test for Shear Resistance of Framed Walls for Buildings." West Conshohocken, PA.: American Society for Testing and Materials.

ASTM F3125 (2019). "Standard Specification for High Strength Structural Bolts and Assemblies, Steel and Alloy Steel, Heat Treated, Inch Dimensions 120 ksi and 150 ksi Minimum Tensile Strength, and Metric Dimensions 830 MPa and 1040 MPa Minimum Tensile Strength." West Conshohocken, PA.: American Society for Testing and Materials.

Data, A. P. (2012). "AISI Standard for Cold-Formed Steel Framing-Product Data 2012 Edition." Washington, D.C.: American Iron and Steel Institute.

FEMA P695 (2009). "Qualifications of Building Seismic Performance Factors." Washington, D.C.: Federal Emergency Management Agency.

IBC (2015). International Building Code, 2015 Edition. Washington, D.C.: International Code Council.

Leng, J. (2015). "Simulation of Cold-formed Steel Structures. Baltimore." MD: PhD Dissertation, Johns Hopkins University.

Mahdavian, M. (2016). "Innovative Cold-Formed Steel Shear Walls with Corrugated Steel Sheathing." Denton, TX: Thesis, University of North Texas.

McKenna, F. e. (2015). "Open system for earthquake engineering simulation (OpenSees)." Berkeley, CA: Pacific Earthquake Engineering Research Center.

OpenSees. PEER, (2021). Berkeley, CA.

Schafer, B.W., Ayhan, D., Leng, J., et al. (2016). "Seismic Response and Engineering of Cold-formed Steel Framed Buildings." Structures, 8: 197-212.

Stojadinovic and Tipping (2007). "Structural testing of corrugated sheet steel shear walls." Ontario, CA: *Report submitted to Charles Pankow Foundation.*

Yu, C., Huang, Z., Vora, H. (2009). "Cold-Formed Steel Framed Shear Wall Assemblies with Corrugated Sheet Steel Sheathing." *Proceedings of the Annual Stability Conference*. Phoenix, AZ: Structural Stability Research Council.

Yu, C. (2013). "Cold-Formed Steel Framed Shear Wall Sheathed with Corrugated Steel Sheet." Denton, TX: Thesis, University of North Texas.

Yu, C., Yu, G. (2016). "Experimental Investigation of Cold-Formed Steel Framed Shear Wall using Corrugated Steel Sheathing with Circular Holes." *ASCE, Journal of Structural Engineering,* Vol. 142, Issue 12, December 2016.

Zhang, W. Mahdavian, M., Li, Y., and Yu, C. (2017a). "Experiments and Simulations of Cold-Formed Steel Wall Assemblies Using Corrugated Steel Sheathing Subjected to Shear and Gravity Loads." *Journal of Structural Engineering*, Vol. 143, Issue 3.

Zhang, W. Mahdavian, M., Li, Y., and Yu, C.(2017b). "Seismic Performance Evaluation of Cold-Formed Steel Shear Walls Using Corrugated Sheet Sheathing." J*ournal of Structural Engineering*, 143(0401715111).

Zhang, W., Mahdavian, M., Lan, X., and Yu, C. (2021). "Cold-Formed Steel Framed Shear Walls with In-Frame Corrugated Steel Sheathing." *J. Struct. Eng.*, 147(12).